region of interest, the small split valence basis set is rather limited. We believe, however, that the high-temperature thermochemistry will be dominated not by the small (~1 kcal) dips and humps in the diradical region but rather by the larger entropic effects. These should survive a better basis set.

The importance of entropy is illustrated in Figure 1, an idealized contour representation of the cis-trans isomerization and fragmentation processes that displays the qualitative features of our surface, though not itself the result of ab inito calculations. Both saddle points are located in the flat biradical plateau region of the surface. This is a region of high entropy associated with the loose modes. From the plateau region, a biradical can form products only by exiting through narrow channels, a restriction that reduces the entropy. The lower potential energy at the entrances to the product channels is more than offset by an increased zero-point energy and reduced entropy. A biradical in the plateau region is therefore trapped by entropic barriers.

There is reason to suspect that the model of an entropy-looked biradical intermediate is not limited to tetramethylene. In many cases, leaving the biradical region of a potential energy surface implies the formation of a new bond together with increasing hindrance to internal rotation. For larger open-chain biradicals in particular, the greater number of internal rotations suggests an even more pronounced entropic effect than in tetramethylene.

Acknowledgment. This work was partially supported by the National Science Foundation (Grant CHE7901138). We are greatly indebted to Dr. Heinrich Martens, director of University Computer Services, for allowing us extraordinary access to the SUNYAB Control Data CYBER 730.

Registry No. Tetramethylene, 287-23-0.

(17) See: Herzberg, G. "Infrared and Raman Spectra of Polyatomic Molecules; Van Nostrand: New York, 1945. The internal rotations were treated separately according to: Pitzer, K.; Gwinn, W. *J. Chem. Phys.* **1942**, *10*, 428. Benson, S. W. "Thermochemical Kinetics", 2nd ed.; Wiley: New York, 1976. For **3** the mass-weighted gradient was project out.

Crystal and Molecular Structure of an *N*-Arylporphyrin Complex: Chloro(*N*-phenyl-5,10,15,20-tetraphenylporphinato)-zinc(II)

Debasish Kuila and David K. Lavallee*

Department of Chemistry
Hunter College of the City University of New York
New York, New York 10021

Cynthia K. Schauer and Oren P. Anderson*

Department of Chemistry, Colorado State University
Fort Collins, Colorado 80523

Received August 9, 1983

In 1885 Hoppe-Seyler reported that the addition of phenylhydrazine to red blood cells led to the formation of aggregated particles ("Heinz bodies") that resemble aggregates characteristic of malarial patients.[1] Recently, Ortiz de Montellano and others have found that *N*-phenylporphyrins are formed by the reaction of phenylhydrazine with hemoglobin or myoglobin under aerobic conditions in the presence of acid,[2] with formation of σ-phenylprotohemin[3] as an intermediate. The formation of other N-substituted porphyrins from biological sources has also been reported. A variety of *N*-alkylporphyrins are formed from the protoheme prosthetic groups of cytochrome P-450 enzymes in the liver of mice after their exposure to simple alkenes or to one of a number of drugs.[4] The isolation and identification of these porphyrins was a consequence of the fact that they inhibit heme biosynthesis and cause readily observable changes in the animals (the drugs had been used for several years to study heme biosynthesis disorders before the *N*-alkylporphyrins products were observed). Their effect on the heme biosynthetic pathway has been verified by direct administration of the *N*-alkylporphyrin to the animal.[5] In this first report of the molecular structure of an *N*-arylporphyrin complex, that of chloro(*N*-phenyl-5,10,15,20-tetraphenylporphinato)zinc(II), we will describe major structural features and compare parameters of the coordination site and the porphyrin ring topology with those of the corresponding *N*-methyl complex of zinc(II) and those of other *N*-methylporphyrin complexes.

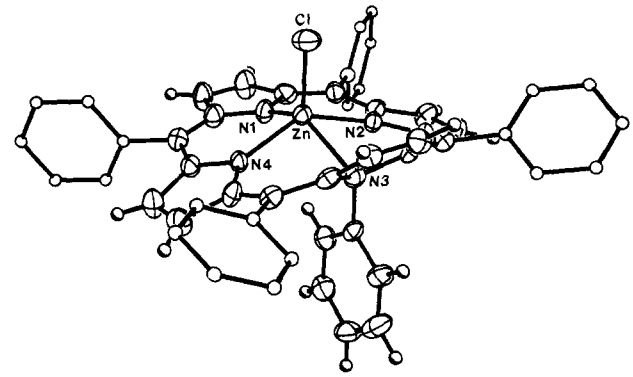

Figure 1. View of the Zn(*N*-Ph(TPP))Cl complex. Hydrogen atoms on the meso phenyl rings have been omitted for clarity, and the thermal ellipsoids that are shown are drawn at the 50% probability level. The complex is almost bilaterally symmetric about the plane of the *N*-phenyl ring.

The metal complexes of *N*-alkylporphyrins show striking similarities to one another. The molecular structures of *N*-methyl-5,10,15,20-tetraphenylporphyrin with Mn(II), Fe(II), Co(II), and Zn(II)[6] have differences that are predictable from bond lengths known from other metalloporphyrin structures[7] and the ionic radius of the particular metal ion.[6d] The highly similar visible absorption spectra of these complexes indicate a decrease in the sensitivity of the $\pi \rightarrow \pi^*$ electronic energy level difference to d subshell occupation in comparison with spectra of corresponding non-N-alkylated porphyrin complexes.[8] In like manner, complexes of *N*-methyldeuteroporphyrin IX dimethyl ester (*N*-CH_3(DP))[9] and *N*-methylprotoporphyrin IX dimethyl ester (*N*-CH_3(PP))[10] exhibit spectra that are more similar to one another than are those of complexes of deuteroporphyrin IX dimethyl ester and protoporphyrin IX dimethyl ester.

The coordination geometry and the topology of the porphyrin ring of chloro(*N*-(ethylacetoxy)octaethylporphinato)cobalt(II)[11]

(1) (a) Hopper-Seyler, G. Z. *Physiol. Chem.* **1885**, *9*, 34-39. (b) Heinz, R. *Virchows Arch. Pathol. Anat. Physiol. Klin. Med.* **1890**, *122*, 112-116.

(2) (a) Ortiz de Montellano, P. R.; Kunze, K. L. *J. Am. Chem. Soc.* **1981**, *103*, 6534-6536. (b) Saito, S.; Itano, H. A. *Proc. Natl. Acad. Sci. U.S.A.* **1981**, *78*, 5508-5512. (c) Augusto, O.; Kunze, K. L.; Ortiz de Montellano, P. R. *J. Biol. Chem.* **1982**, *257*, 6231-6241.

(3) (a) Kunze, K. L.; Ortiz de Montellano, P. R. *J. Am. Chem. Soc.* **1983**, *105*, 1380-1381. (b) Battioni, P.; Mahy, J.-P., Gillet, O.; Mansuy, D. *Ibid.* **1983**, *105*, 1359-1401.

(4) (a) Ortiz de Montellano, P. R.; Kunze, K. L.; Mico, B. A. *Mol. Pharmacol.* **1980**, *18*, 602-605. (b) Tephly, T. R.; Coffman, B. L.; Ingall, G.; Abou-Zeit-Har, M. S.; Gofa, H.; Tobba, H. O.; Smith, K. M. *Arch. Biochem. Biophys.* **1981**, *212*, 120-126. (c) De Matteis, F.; Hollands, G.; Gibbs, A. H.; DeSa, N.; Rizzardini, M. *FEBS Lett.* **1982**, *145*, 87-92.

(5) (a) Tephly, T. R.; Gibbs, A. H.; De Matteis, F. *Biochem. J.* **1974**, *180*, 241-244. (b) De Matteis, F.; Gibbs, A. H.; Tephly, T. R. *Ibid.* **1980**, 145-152.

(6) (a) Anderson, O. P.; Lavallee, D. K. *J. Am. Chem. Soc.* **1977**, *99*, 1404-1409. (b) Anderson, O. P.; Lavallee, D. K. *Inorg. Chem.* **1977**, *16*, 1634-1640. (c) Lavallee, D. K.; Kopelove, A. B.; Anderson, O. P. *J. Am. Chem. Soc.*, **1980**, *100*, 3025-3033. (d) Anderson, O. P.; Kopelove, A. B.; Lavallee, D. K. *Inorg. Chem.* **1980**, *19*, 2101-2107.

(7) Hoard, J. L. In "Porphyrins and Metalloporphyrins"; Smith, K. M., Ed.; Elsevier: Amsterdam, 1975; p 317 ff.

(8) Lavallee, D. K. *Bioinorg. Chem.* **1976**, *6*, 219-227.

(9) Lavallee, D. K.; Bain-Ackerman, M. J. *Bioinorg. Chem.* **1978**, *9*, 311-321.

(10) Lavallee, D. K. *J. Inorg. Biochem.* **1982**, *16*, 135-143.

(11) Goldberg, D. E.; Thomas, K. M. *J. Am. Chem. Soc.* **1976**, *98*, 913-919.

0002-7863/84/1506-0448$01.50/0

Table I. Visible Absorption Spectra of Some *N*-Alkyl- and *N*-Phenylporphyrins and Their Complexes[a]

species	absorption maxima, nm	species	absorption maxima, nm
N-PhH(TPP)	442, 550, 596, 635, 703	Zn(*N*-Ph(TPP))Cl	447, 459, 567, 628, 680
N-CH_3H(TPP)[b]	432, 534, 575, 613, 676	Zn(*N*-CH_3(TPP))Cl	439, 448, 561, 611, 658
N-CH_2CH_3H(TPP)[b]	432, 531, 573, 613, 675	Zn(*N*-Ph(PP))Cl[c]	442, 550, 606, 648
N-($CH_2CO_2C_2H_5$)H(TPP)[b]	432, 531, 572, 615, 676	Zn(*N*-CH_3(PP))Cl[c]	429, 546, 591, 633
N-(*p*-$CH_2C_6H_4NO_2$)H(TPP)[b]	432, 529, 570, 613, 675	Fe(*N*-Ph(TPP))Cl[d]	454, 465, 570, 630, 681
N-PhH(PP)[c]	430, 518, 550, 613, 670	Fe(*N*-CH_3(TPP))Cl[d]	447, 459, 564, 610, 662
N-CH_3H(PP)[c]	417, 510, 546, 594, 650	Fe(*N*-C_2H_5(TPP))Cl[d]	446, 457, 563, 612, 662

[a] At ambient temperature in CH_2Cl_2 except as noted. See text for abbreviations. [b] These complexes also show a prominent shoulder at 497 nm. [c] These species consistent of isomers with similar but not identical spectra, see ref 4a. [d] In tetrahydrofuran.

Table II. Proton NMR Chemical Shifts of Some *N*-Alkyl- and *N*-Phenylporphyrins and Complexes in the β-Pyrrole Region[a]

	δ (relative to Me_4Si)[b]					δ (relative to Me_4Si)			
species	s (2 H)	d (2 H)	d (2 H)	s (2 H)	species	s (2 H)	d (2 H)	d (2 H)	s (2 H)
N-CH_3H(TPP)[c] (*N*-CH_3, −4.16)	8.86	8.60	8.52	7.48	Zn(*N*-CH_3(TPP))Cl[d] (*N*-CH_3, −3.98)	8.80	8.97	8.90	8.36
N-C_2H_5H(TPP)	8.81	8.70	8.49	7.50					
N-($CH_2CO_2C_2H_5$)H(TPP)	8.78	8.66	8.46	7.64					
N-(*p*-$CH_2C_6H_4NO_2$)H(TPP)	8.87	8.61	8.51	7.59					
N-PhH(TPP)[c] (*N*-phenyl, ortho, 2.99; meta, 5.20; para, 5.67)	8.70	8.33	8.16	7.35	Zn(*N*-Ph(TPP))Cl[d] (*N*-phenyl, ortho, 2.36; meta, 5.22; para, 5.76)	8.92	8.74	8.66	8.48

[a] In $CDCl_3$, using Varian 200-MHz instrument unless otherwise cited. [b] For assignments, see text. [c] Reference 5b. [d] In CD_2Cl_2.

are similar to those of Co(*N*-CH_3TPP)Cl. The absorbance spectra of copper(II) complexes of *N*-methyl-, *N*-ethyl-, and *N*-benzyltetraphenylporphyrin closely resemble each other.[12] Both of these features indicate that the porphyrin ring topoloby is likely to be similar for both meso-substituted and unsubstituted *N*-alkylporphyrin complexes in which the first functional group bound to the pyrrolic nitrogen atom is a sp^3 hybridized carbon atom (a methyl group or methylene moiety in the cases cited above).

Features of the visible absorption and NMR spectra of *N*-phenylporphyrins and their complexes are distinct from those of the *N*-alkylporphyrins. Absorption maxima for the *N*-phenyl species are characteristically at longer wavelengths (typically 10–20 nm) than those of corresponding N-alkylated species (Table I). Differences are evident in the β-pyrrolic hydrogen atom chemical shifts between the free ligands *N*-CH_3H(TPP) and *N*-PhH(TPP). There are also similar differences between the corresponding chlorozinc(II) complexes (Table II). In addition, the basicity of *N*-phenyltetraphenylporphyrin is somewhat greater than that of *N*-methyltetraphenylporphyrin (a pK_a of 9.7 for formation of *N*-$PhH_2(TPP)^+$ and 3.5 for formation of *N*-$PhH_3(TPP)^{2+}$ vs. 7.7 for formation of *N*-$CH_3H_2(TPP)^+$ and 2.6 for formation of *N*-$CH_3H_3(TPP)^{2+}$).[13]

The structural parameters we now report for chloro(*N*-phenyl-5,10,15,20-tetraphenylporphinato)zinc(II) (Zn(*N*-Ph(TPP))Cl)[14] provide a basis for assessing the origins of these observed differences. From Figure 1, it can be seen that in the solid state the *N*-phenyl group is poised so that one ortho hydrogen atom is near the zinc atom (Zn–H = 2.52 Å, while Zn–Cl is only 0.3 Å shorter at 2.24 Å) and the other ortho hydrogen atom is below the substituted pyrrole ring. The NMR spectrum of this species from room temperature to −56 °C (in $CDCl_3$, 2.36 (d, 2 H), 5.22 (d, 2 H), and 5.76 (t, 1 H)ppm) indicates that the two ortho hydrogen atoms are equivalent on the NMR time scale. The observed solid-state structure (see Figure 1) indicates the possibility of such rotation. The largest change of the phenyl NMR chemical shifts on complex formation is, as expected, that assigned to the ortho hydrogen atoms (Table II). In addition to the position of the *N*-phenyl substituent, an important feature of this structure is the cant of the substituted pyrrole ring relative to the plane of the three non-alkylated nitrogen atoms. In the structure of the *N*-phenyl complex, this angle is 42.0°, while for the *N*-CH_3(TPP) complexes the angle is 29.2° (Mn(II)),[6b] 28.9° (Fe(II)),[6d] 31.6° (Co(II)),[6a] and 38.5° (Zn(II)),[6c] with the order of increase in angle in the same order as the increase in length of the M–*N*-CH_3 bond. The comparable angle for the free base *N*-$CH_3Br_4H(TPP)$ is 27.7°.[15] Other features of the structure of Zn(*N*-CH_3(TPP))Cl and the present structure are closely related: the distance of the zinc atom from the plane of the three non-alkylated nitrogen atoms (0.65 and 0.67 Å, respectively), the deviation of the zinc atom from the plane formed by the substituted pyrrole ring (2.04 vs. 2.12 Å), and the zinc–nitrogen bond distances (Zn–NR 2.530 vs, 2.499 Å, Zn–N (adjacent rings) 2.089 vs. 2.086 Å and 2.081 vs. 2.102 Å, and Zn–N (opposite ring), 2.018 vs. 2.015 Å). These structural features are quite consistent with the NMR spectra of Zn(*N*-PhTPP)Cl and Zn(*N*-CH_3(TPP))Cl. Although the spectra of these complexes are quite different in the β-pyrrolic hydrogen region, the differences between the complexes are comparable to differences between the ligands (Table II), indicating that the phenyl group exerts a rather similar effect relative to the methyl group in both cases. The most shielded singlet in this region is assigned to the β-H atoms most removed from the plane of the ring current. The zinc atom is 2.04 or 2.14 Å, respectively, from the plane of the substituted pyrrole ring. At this distance, it may exhibit a through-space effect on the β-H shielding. In both cases, the β-H singlet is shifted downfield by 0.9 ppm or more on complexation to either *N*-alkylporphyrins or the *N*-Ph(TPP) species (Table II). Doublets due to the β-H atoms of the adjacent pyrrole rings (one assigned to protons 7 and 18, the other to 8 and 17) are shifted comparably on complexation of Zn(II). The singlet assigned to the β-H atoms of the opposed ring are much less shifted, perhaps due to the change of orientation of this ring upon

(12) Lavellee, D. K.; Kuila, D. *Inorg. Chem.*, submitted for publication.

(13) The pK_a values were determined in 80/20 v/v Me_2SO/H_2O (buffered) using spectrophotometric titrations. The observed pH values (Radiometer Model 84 meter, calibrated with pH 4.0 aqueous buffer) were converted to the reported values using the method described in: Westcott, C. C. "pH Measurements"; Academic Press: New York, 1979; pp 109–138.

(14) The complex was synthesized from *N*-phenyl-5,10,15,20-tetraphenylporphine (made from ClFe(TPP) by the method of Ortiz de Montellano[4a] with the exception that phenyllithium was used in place of phenylmagnesium bromide) and hydrated zinc chloride in acetonitrile. Crystals were obtained after repeated recrystallization from a mixture of CH_3CN and CH_2Cl_2. For $ZnCl(C_{50}H_{33}N_4)$: orthorhombic, space group $P2_12_12_1$; a = 15.078 (5) Å, b = 15.272 (5) Å, c = 17.268 (5) Å; ρ_c = 1.32 g cm^{-3} (Z = 4, M_r = 790.63), ρ_m = 1.30 g cm^{-3}. No absorption correction was performed (the data collection crystal measured 0.37 mm × 0.47 mm × 0.15 mm, μ = 7.4 cm^{-1}). The intensities of 2928 unique, observed ($I > 2\sigma(I)$) reflections were determined by θ–2θ scans on the Nicolet R3m/E diffractometer (Mo Kα radiation). The final structural model involved anisotropic thermal parameters for all nonhydrogen atoms, idealized rigid phenyl rings, and hydrogen atoms placed in idealized, fixed positions. This model refined to convergence with R = 0.055, R_w = 0.057, and GOF = 1.20.

(15) Lavallee, D. K.; Anderson, O. P. *J. Am. Chem. Soc.* **1982**, *104*, 4707–4708.

complexation,[6,15] which could lead to a cancellation of effects.

The structure of the *N*-phenylporphyrin complex, Zn(*N*-PhTPP)Cl, shows that the phenyl ring is relatively unhindered and free to rotate as indicated from its NMR spectrum. The N-C(phenyl) bond distance of 1.491 Å indicates a strong bond, consistent with the finding that *N*-phenylporphyrins show an unusually high stability against removal of the N substituent.[12] The structure of the coordination site and the porphyrin ring topology are closely related to those of the corresponding *N*-methyl complex,[6c] suggesting that the metal-nitrogen bond lengths and the cant of the pyrrole rings may be determined principally by the metal ion rather than the nitrogen-bound substituent. The comparison of Zn(II) complexes, however, may be misleading since the Zn-NR bond distance is long.[6c] A comparison of structures involving metals that form a stronger M-NR bond (such as Fe(II)[6d] or Mn(II)[6b]) would establish this point. The differences in spectral properties between *N*-phenyl- and *N*-alkylporphyrins and their complexes appear to be due to electronic rather than structural differences.

Acknowledgment. We are grateful for support of the NIH (CA 25457) and the PSC-BHE grants program of the City University of New York. The Nicolet R3m/E X-ray diffractometer and computing system at Colorado State University was purchased with funds provided by the NSF (CHE 8103011). We thank A. Sudhakar with assistance in obtaining NMR spectra.

Registry No. *N*-PhH(TPP), 81856-91-9; *N*-CH_3H(TPP), 51552-53-5; *N*-CH_2CH_3H(TPP), 73568-09-9; *N*-$(CH_2CO_2C_2H_5)$H(TPP), 53226-50-9; *N*-$(p\text{-}CH_2C_6H_4NO_2)$H(TPP), 80641-51-6; Zn(*N*-Ph(TPP))Cl, 84079-98-1; Zn(*N*-CH_3(TPP))Cl, 59765-81-0; Fe(*N*-Ph(TPP))Cl, 83219-61-8; Fe(*N*-CH_3(TPP))Cl, 64813-94-1; Fe(*N*-C_2H_5(TPP))Cl, 88376-67-4.

Supplementary Material Available: Table I, listing atomic coordinates and U_{iso} for non-hydrogen atoms of Zn(*N*-Ph(TPP))Cl (1 page). Ordering information is given on any current masthead page.

Oxygen-17 NMR and Oxygen-18-Induced Isotopic Shifts in Carbon-13 NMR for the Elucidation of a Controversial Reaction Mechanism in Carbohydrate Chemistry

Aimée Dessinges, Sergio Castillon, Alain Olesker, Ton That Thang, and Gabor Lukacs*

Institut de Chimie des Substances Naturelles du CNRS 91190 Gif-sur-Yvette, France

Received August 2, 1983

The formation of 1,4-anhydro-6-azido-2,3-di-*O*-benzoyl-6-deoxy-β-D-galactopyranose (**3a**) from 1-*O*-acetyl-2,3-di-*O*-benzoyl-4,6-bis-*O*-(methylsulfonyl)-α-D-glucopyranose (**1b**) by treatment with sodium azide was suggested to proceed by way of a ring contraction process (Figure 1, pathway a).[1] Subsequently, an alternative mechanism was proposed, pathway b, for the formation of **3a** and closely related 1,4-anhydro sugars.[2] According to pathway b, the reaction is initiated by attack at the

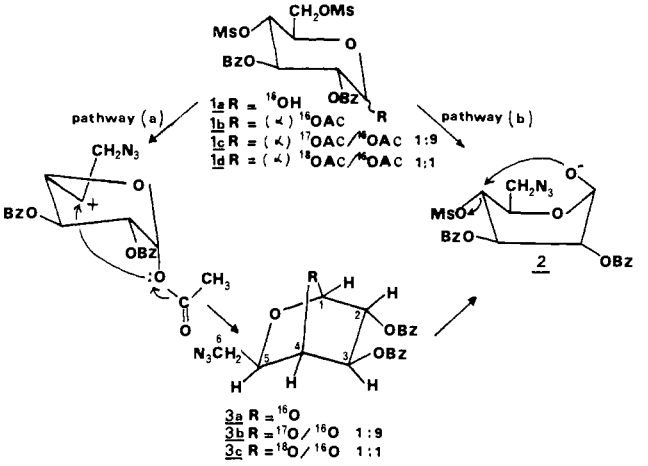

Figure 1.

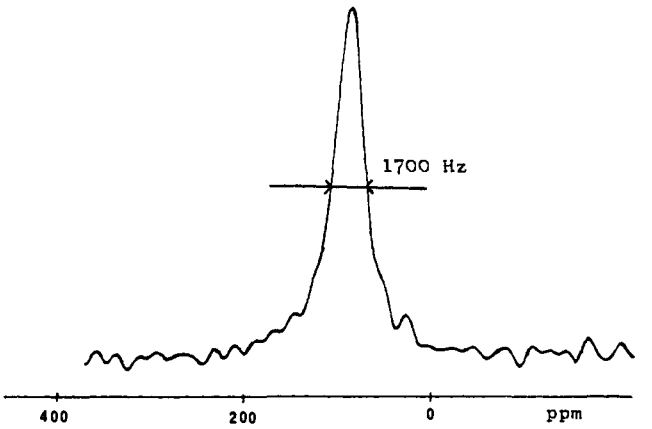

Figure 2. ^{17}O NMR spectrum of 1,4-anhydro-6-azido-2,3-di-*O*-benzoyl-6-deoxy-β-D-galactopyranose-1,4-^{17}O (**3b**) (about 10% enrichment), measured at 53.6 °C, at 48.8 MHz on a WH-360 Bruker spectrometer on a 27-mg sample in 1.5 mL of $CHCl_3$. The chemical shift of the labeled oxygen atom is 85.9 ppm relative to external 1,4-dioxane with an estimated error of ±0.5 ppm. The natural abundance ^{17}O signals are not observed. T_{acq} = 2 ms, NS = 200 000, line width at half-height = 1700 Hz. Neither field frequency lock nor Guassian resolution enhancement was used.

acetyl carbonyl atom followed by anomerization of the derived C-1 oxy anion **2**, which then displaces the methylsulfonyl group from C-4 (Figure 1).[2] In the case of pathway b, C-4 becomes attached to the anomeric oxygen atom O-1 while the contraction procedure shown in pathway a requires C-4 to be bonded to the ring oxygen atom O-5. In order to elucidate the mechanism of this reaction, Ferrier suggested the necessity for its reinvestigation.[3] With the help of oxygen-17 NMR spectroscopy[4] and oxygen-18-induced isotopic shifts in carbon-13 NMR,[5] we present evidence here for the mechanism of the formation of the trisubstituted 2,7-dioxanorbornane structure **3a** according to pathway b. The techniques used appear to be the first structural applications to carbohydrate chemistry.

Oxygen-17 NMR spectroscopy has found only very limited applications in organic chemistry as a result of the low natural abundance (0.037%) and sensitivity of this isotope ($I = {}^5/_2$).[4] Difficulties are also associated with an appreciable electric quadrupole moment of ^{17}O ($Q = -2.6 \times 10^{-26}$ cm^2) and large field gradients, inducing broad lines in medium-sized organic molecules. In spite of these problems the ^{17}O NMR chemical shifts of a number of monosaccharide derivatives were recently assigned from specifically labeled[6] and even from natural abundance samples.[7] The O-5 ether oxygen NMR signal of the hexopyranoses or hexopyranosides studied in the chair conformation

(1) Bullock, C.; Hough, L.; Richardson, A. C. *J. Chem. Soc., Chem. Commun.* **1971**, 1276.
(2) Brimacombe, J. S.; Minshall, J.; Tucker, L. C. N. *J. Chem. Soc., Chem. Commun.* **1973**, *142*; *J. Chem. Soc. Perkin Trans. 1* **1973**, 2691.
(3) Ferrier, R. J. In "MTP International Review of Science-Carbohydrates"; Aspinall, G. O., Ed.; Butterworths: London, 1976; p 40.
(4) (a) Klemperer, W. G. *Angew. Chem., Int. Ed. Engl.* **1978**, *17*, 246. (b) Kintzinger, J.-P. In "NMR Basic Principles and Progress"; Diehl, P., Fluck, E., Kosfeld, R., Eds.; Springer-Verlag: Berlin, 1981; Vol. 17, p 1.
(5) (a) Risley, J. M.; Van Etten, R. L. *J. Am. Chem. Soc.* **1979**, *101*, 252. (b) Verderas, J. C. *Ibid.* **1980**, *102*, 374.
(6) Gorin, P. A. J.; Mazurek, M. *Carbohydr. Res.* **1978**, *67*, 479.
(7) Gerothanassis, I. P.; Lauterwein, J. *Sheppard*, N. *J. Magn. Reson.* **1982**, *48*, 431.
(8) Sugawara, T.; Kawada, Y.; Katoh, M.; Iwamura, H. *Bull. Soc. Chim. Jpn.* **1979**, *52* (11), 3391.

0002-7863/84/1506-0450$01.50/0